

Performance Analysis and Optimization of Cooperative Full-Duplex D2D Communication Underlying Cellular Networks

Guoling Liu, Wenjiang Feng, Zhu Han, *Fellow, IEEE*,
and Weiheng Jiang, *Member, IEEE*

Abstract

This paper investigates the cooperative full-duplex device-to-device (D2D) communication underlying a cellular network, where the cellular user (CU) acts as a full-duplex relay to assist the D2D communication. To simultaneously support D2D relaying and uplink transmission, superposition coding and successive interference cancellation are adopted at the CU and the D2D receiver, respectively. The achievable rate region and joint outage probability are derived to characterize the performance of the considered system. An optimal power allocation scheme is proposed to maximize the minimum achievable rate. Besides, by analyzing the upper bound of the joint outage probability, we study a suboptimal power allocation to improve the outage performance. The simulation results confirm the theoretical analysis and the advantages of the proposed power allocation schemes.

Index Terms

Full-duplex communication, D2D, superposition coding, successive interference cancellation, power allocation.

I. INTRODUCTION

To meet the booming data demand of emerging wireless communication services, researchers in academia and industry are seeking for new technologies to reform the traditional cellular

G. Liu, W. Feng and W. Jiang are with the College of Communication Engineering, Chongqing University, Chongqing, 400044 China (e-mail: {liuguoling, fengwj, whjiang}@cqu.edu.cn).

Z. Han is with the Department of Electrical and Computer Engineering, University of Houston, Houston, TX 77004 USA, and also with the Department of Computer Science, University of Houston, Houston, TX 77004 USA (e-mail: zhan2@uh.edu).

networks. As an attractive candidate, device-to-device (D2D) communication [1] underlying cellular networks draws wide attention. By allowing direct communication between proximal users without traversing the base station (BS) or core network, D2D communication provides improvement in spectrum efficiency, energy efficiency and communication delay, and thus enables high-rate proximity-aware services, such as media sharing, social network and gaming [2]. Consequently, D2D communication is considered as a promising technology in the next generation wireless network [3].

A. Background of Cooperative D2D and Full-Duplex Communication

Although D2D communication can support high spectrum efficiency, the actual transmission rate of D2D users is restricted by practical constraints, such as modulation and coding schemes. Therefore, the channel capacity of D2D links is insufficiently utilized [4]. To address the redundant capacity problem, cooperation is introduced to D2D communication for coverage extension and performance enhancement of the cellular networks. Reference [5] allows a D2D transmitter (DT) to act as a relay to assist the downlink cellular transmission and at the same time transmit its own data to a D2D receiver (DR) by employing superposition coding (SC) [6]. The cellular user performs maximum-ratio-combining to decode the data from the BS and DT. And the DR uses successive interference cancellation (SIC) [7] to decode the D2D data. Therefore, both the cellular and D2D users can benefit from cooperation. The same cooperation scheme is also investigated in the cellular uplink and overlay D2D scenario [8], where the employment of SC is replaced by orthogonal radio source allocation for simultaneous cellular and D2D communication. In [9], the authors assign the DT as a two-way relay to establish a bidirectional cellular link while communicating with a DR. A relay selection method is proposed to achieve a larger rate region. The limited battery lifetime of D2D users is considered in [10], [11]. The authors use auction game to modelled the resource allocation problems, and proposed corresponding auction algorithms to optimized the energy efficiency.

The aforementioned researches focus on the half-duplex (HD) cooperation, which suffers a loss of spectrum efficiency. Recently, the in-band full-duplex (FD) cooperation [12], [13], [14] is a frequent topic. With the breakthrough of self-interference suppression (SIS), simultaneous transmission and reception in the same frequency band becomes practical in realistic wireless networks. The deployment of FD communication may overcome the loss of spectrum efficiency due to HD cooperation. However, the main shortcoming of FD communication is the residual

self-interference (RSI) [15] caused by imperfect SIS. The feasibility and superiority of FD communication in non-cooperative D2D networks has been demonstrated in [16], [17], [18]. In [19], the FD DT cooperates with the BS to perform non-orthogonal multiple access (NOMA) [20] and improves the outage performance of the user with weak cellular downlink. An adaptive multiple access switching method is proposed to dynamically choose the optimal multiple access scheme. As a dual-hop version of the model in [19], Zhang *et al.* investigate the optimal power allocation to minimize the outage probability [21]. To address the fairness issue between the NOMA-strong and NOMA-weak user, another power allocation scheme is studied to maximize the minimum rate achieved by the cellular and D2D link. Reference [22] considers the same cooperative scheme as in [5] with the DT operating in the FD mode. The cellular and D2D data are superposed in different power levels at the DT. Under the aggregate power constraint, an optimal power allocation algorithm is designed to maximize the achievable rates for the D2D users while fulfilling the minimum rate requirements of the cellular users. However, there is no SIC employed at the receiver of the cellular user and DR to deal with the mutual interference, which can be unsubstantial in some circumstances. The same model with amplify-and-forward relaying is discussed in [23]. A D2D based multicast service is considered in [24], one FD user equipment (UE) helps the BS convey data to a group of UEs. The FD D2D based multicast protocol has higher power efficiency than existing schemes, but the group size is limited to two UEs.

B. Motivation and Related Work

All the works in [19], [21], [22], [23], [24] consider that there is always a direct link between DT and DR. When the DT and DR are separated far away from each other or the D2D link has poor quality, the D2D users either abandon the transmission or resort to the BS for data relaying [4], which limits the advantage of the D2D communication. To this end, relay-aided D2D communication becomes an urgent topic. Under the background of HD relaying, many works, including performance analysis [25], [26], relay selection [27], mode selection [28], resource allocation [29], [30], [31] and energy saving [32], etc., are devoted to the investigation of relay-aided D2D communication. By introducing FD relaying, the performance of relay-aided D2D network can be further improved. In [33], Dang *et al.* design a dual-hop FD relay-assisted D2D scheme underlying a cellular uplink transmission and propose a suboptimal power allocation scheme to minimize the outage probability of the D2D under aggregate power constraint of

the DT and the relay. The quality-of-service (QoS) of the cellular user is provisioned by the power control method at the DT. Subsequently, this work is extended to a multi-user OFDMA scenario [34]. The relay selection problem in cooperative D2D networks is considered in [35]. A matching theory based relay selection method is proposed to minimize the power consumption of D2D users.

In aforementioned works, the coverage extension and performance improvement of the D2D communication are implemented through an extra relay node (acted by an idle D2D user or a dedicated relay). As shown in the literature, this relay node complicates the interference between the cellular and the D2D link, and requires more sophisticated interference manage technology. As a supplement to existing researches, we aim to ameliorate the relay-aided D2D networks from the following aspects. Firstly, the FD relaying is employed to increase the spectrum efficiency. Secondly, we consider the cooperation between the D2D and the cellular users to cope with the interference caused by data relaying. Thirdly, we jointly optimize the performance of both the cellular and the D2D users by the resource allocation method.

C. Our Contributions

Inspired by existing works, we propose a new cooperative D2D scheme where the uplink cellular user (CU) acts as an FD decode-and-forward relay between a pair of D2D users, taking RSI at the CU and power control at the DT into account. The CU employs NOMA to support concurrent uplink and D2D communication. Specifically, the CU superimposes the uplink and D2D data with different power levels, and then broadcasts the superposed data to the BS and the DR. The BS and the DR extract their desired data according to a predefined decoding order. The contributions of this paper are summarized as follows.

- 1) *Performance Analysis*: We present the achievable rate region of the cellular uplink rate versus the dual-hop D2D link rate. The Pareto boundary of the region is founded by jointly optimizing the transmit power and power splitting factor at the CU. Besides, we analyse the exact and asymptotic expressions of the joint outage probability of the cellular and D2D link.
- 2) *Power Allocation*: Two power allocation schemes are studied in this paper. In consideration of fairness between the cellular and cooperative D2D communication, a maximization problem of minimum achievable rate is formulated at first. Then, due to the intractability of the exact joint outage probability, we derive its upper bound and formulate a relaxed

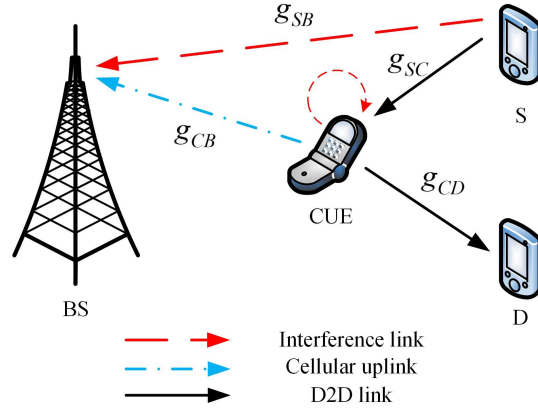


Fig. 1: System model of cooperative full-duplex D2D communication underlying a cellular network.

minimization problem of joint outage probability. Both optimization problems are proved to be quasi-concave and have unique solutions.

- 3) *Simulation and Discussion*: We use Monte Carlo simulation to validate the correctness of performance analysis and the advantage of the proposed power allocation schemes. In the end, we illustrate the impact of RSI on the network performance and compare with the HD network.

D. Organization

The rest of this paper is organized as follows. Section II presents the system model and fundamental assumptions. Detailed analyses of achievable rate region and joint outage probability are provided in Section III. In Section IV, we analyzed the maximization problem of the minimum achievable rate. The relaxed minimization problem of joint outage probability is investigated in Section V. Simulation results and discussions are shown in Section VI. In the end, we conclude this paper in Section VII.

II. SYSTEM MODEL

As shown in Fig. 1, the proposed cooperative FD D2D system consists of one BS, one FD CU, one pair of HD DT and DR, which are denoted as B, C, S and D, respectively. In each transmission period, the CU sends a message to the BS. Meanwhile, the CU acts as an FD decode-and-forward relay to assist the D2D transmission from S to D. To improve the spectral

efficiency, the cooperative D2D transmission reuses the cellular uplink channel. Each node is equipped with a single antenna. The channel gain between nodes i and j is denoted as g_{ij} , $i, j \in \{B, C, S, D\}$. We consider Rayleigh fading, i.e., $g_{ij} \sim \mathcal{CN}(0, \varphi_{ij})$, where φ_{ij} is the average power gain of the corresponding channel. The direct link between S and D is ignored due to heavy shadowing or path-loss, i.e., $g_{SD} = 0$.

A. Signal Model

1) *Power Control Method*: In order to manage the interference at the BS, the truncated channel inverse power control [36] is adopted at S. The transmit power of S can be expressed as

$$p_S = \min \left(\frac{\theta}{h_{SB}}, P_S \right), \quad (1)$$

where θ is the maximum tolerable interference threshold predefined by the BS, P_S is the maximum transmit power of S, $h_{ij} = |g_{ij}|^2$ denotes the instantaneous power gain of the channel between nodes i and j .

2) *Statistical Model of Residual Self-Interference*: Following the previous work in [37], [38], [39], we model the RSI at the CU, v_C , as an additive and Gaussian random variable,

$$v_C \sim \mathcal{CN}(0, \beta p_C^\lambda), \quad (2)$$

where $p_C \in [0, P_C]$ is the transmit power of the CU, P_C is the maximum transmit power of the CU, $\beta \in [0, +\infty)$ and $\lambda \in [0, 1]$ reflect the performance of SIS. Define the Transmit-power-to-RSI ratio (TRR) as

$$\text{TRR} = \frac{p_C}{\beta p_C^\lambda}. \quad (3)$$

Unlike the RSI model in [19], [21], [22], [23], [24], [33], [34], [35], we can see that the TRR is not constant, but an increasing function of p_C . The RSI model in (2) incorporates two important cases: (i) $\lambda = 0$ indicates a constant RSI level, in this case, the RSI behaves like the noise; (ii) $\lambda = 1$, the RSI grows linearly with p_C , as in the aforementioned researches. As will be shown in the subsequent section, the value of λ has a major influence on the system performance.

3) *Transmission Protocol*: To facilitate the depiction, we divide the transmission protocol into two concurrent phases.

- *Phase-I*: In transmission period t , S sends a message $x_S(t)$ with power p_S to the CU, the received signal at the CU is

$$y_C(t) = \sqrt{p_S} g_{SC} x_S(t) + v_C(t) + n_C(t), \quad (4)$$

where $n_i(t) \sim \mathcal{CN}(0, \sigma_i^2)$ denotes the additive Gaussian white noise (AWGN) at node i .

- *Phase-II*: After decoding $y_C(t)$, the CU forms a broadcasting signal as

$$\bar{x}_C(t) = \sqrt{\alpha p_C} x_C(t) + \sqrt{(1-\alpha)p_C} \hat{x}_S(t-t_0), \quad (5)$$

where $\alpha \in [0, 1]$ is the power splitting factor which represents the proportion of the power allocated to x_C , x_C is the uplink message of the CU, \hat{x}_S is the decoded version of message x_S , and t_0 denotes the processing delay. Therefore, the received signals at the BS and the D2D receiver can be expressed as

$$y_B(t) = g_{CB} \bar{x}_C(t) + n_B(t) \quad (6)$$

and

$$y_D(t) = g_{CD} \bar{x}_C(t) + n_D(t), \quad (7)$$

respectively.

It should be emphasized that the FD nature of the CU makes *Phase-I* and *Phase-II* parallel in time at the cost of self-interference. If the CU operates in the HD mode, two orthogonal channels are required to separate *Phase-I* and *Phase-II*, which reduces the spectral efficiency.

B. SINR model

Conditioning on h_{SB} , the signal-to-interference-plus-noise ratio (SINR) at the CU to decode x_S is

$$\gamma_{SC} = \frac{p_S h_{SC}}{\beta p_C^\lambda + \sigma_C^2} = \begin{cases} \frac{\theta h_{SC}}{h_{SB}(\beta p_C^\lambda + \sigma_C^2)}, & h_{SB} \geq \frac{\theta}{P_S}, \\ \frac{P_S h_{SC}}{\beta p_C^\lambda + \sigma_C^2}, & h_{SB} < \frac{\theta}{P_S}. \end{cases} \quad (8)$$

The decoding order, which has significant impact on the power allocation scheme, plays a key role in the NOMA system. In this paper, we assign the DR to decode \hat{x}_S with SIC. After receiving y_D , the DR first regards \hat{x}_S as the noise and tries to decode x_C . If the decoding is successful, the DR subtracts x_C from y_D and then decodes \hat{x}_S . The SINR at the DR to decode x_C is

$$\gamma_{CD,C} = \frac{\alpha p_C h_{CD}}{(1-\alpha)p_C h_{CD} + \sigma_D^2}, \quad (9)$$

and the signal-to-noise ratio (SNR) to decode \hat{x}_S after SIC is

$$\gamma_{CD,S} = \frac{(1-\alpha)p_C h_{CD}}{\sigma_D^2}. \quad (10)$$

On the other hand, the BS treats x_S and \hat{x}_S as interference and directly decodes x_C , the SINR at the BS is

$$\begin{aligned} \gamma_{CB} &= \frac{\alpha p_C h_{CB}}{p_S h_{SB} + (1 - \alpha) p_C h_{CB} + \sigma_B^2} \\ &= \begin{cases} \frac{\alpha p_C h_{CB}}{\theta + (1 - \alpha) p_C h_{CB} + \sigma_B^2}, & h_{SB} \geq \frac{\theta}{P_S}, \\ \frac{\alpha p_C h_{CB}}{P_S h_{SB} + (1 - \alpha) p_C h_{CB} + \sigma_B^2}, & h_{SB} < \frac{\theta}{P_S}. \end{cases} \end{aligned} \quad (11)$$

III. PERFORMANCE ANALYSIS

In this section, we provide the performance analyses from two perspectives. On one hand, The Pareto boundary of the achievable rate region is calculated along with the corresponding power allocation strategy. On the other hand, we characterize the network performance by the joint outage probability of the cellular uplink and the cooperative D2D links, of which the exact and asymptotic expressions are presented.

A. Achievable Rate Region

For a given power allocation scheme (α, p_C) , we have the achievable rate of the cellular uplink channel from the CU to the BS as

$$R_B(\alpha, p_C) = \log_2(1 + \gamma_{CB}), \quad (12)$$

and the achievable rate of the dual-hop D2D relay channel as

$$R_D(\alpha, p_C) = \min(R_{SC}(p_C), R_{CD,S}(\alpha, p_C)), \quad (13)$$

where

$$R_{SC}(p_C) = \log_2(1 + \gamma_{SC}), \quad (14)$$

$$R_{CD,S}(\alpha, p_C) = \log_2(1 + \gamma_{CD,S}). \quad (15)$$

From (12) and (13), we can see a tradeoff between the achievable rates between the cellular uplink and the cooperative D2D channels. Let us first consider two extreme cases: (i) if $\alpha = 1$, the CU would assign full power (i.e., $p_C = P_C$) for uplink transmission and the D2D link suffers an outage; (ii) if $\alpha = 0$, the CU uses full power to relay the data from the DT to the DR, and the achievable rate of the cellular uplink is zero. Therefore, we have the power allocation schemes $(0, P_C)$ and $(1, P_C)$ at the extreme points of the Pareto boundary of the achievable rate

region. The values of (α, p_C) on the Pareto boundary can be obtained by solving the following optimization problem

$$\begin{aligned} \mathcal{OP}1 : \quad & \max_{\alpha, p_C} R_D(\alpha, p_C) \\ & s.t. \quad R_B(\alpha, p_C) = \tilde{R}_B \\ & \quad \quad 0 \leq \alpha \leq 1, 0 \leq p_C \leq P_C \end{aligned} \quad (16)$$

at an arbitrary achievable rate of the cellular uplink $\tilde{R}_B \in [0, R_B^{\max}]$, where $R_B^{\max} = \log_2 \left(1 + \frac{P_C h_{CB}}{p_S h_{SB} + \sigma_B^2} \right)$ denotes the maximum achievable rate of the cellular uplink. To solve $\mathcal{OP}1$, we provide the following lemma, which will also be used in the rest of this paper.

Lemma 1. *For bounded $x \in (x_{min}, x_{max})$, if $f(x)$ is a bounded, continuous and monotonically increasing function, and $g(x)$ is a bounded, continuous and monotonically decreasing function, $h(x) = \min(f(x), g(x))$ will be quasi-concave.*

Proof. See [33] for the proof of Lemma 1. □

With the help of Lemma 1, we can prove that $\mathcal{OP}1$ is quasi-concave [40], and the solution is offered in Theorem 1.

Theorem 1. *The power allocation $(\tilde{\alpha}, \tilde{p}_C)$ that achieves the Pareto boundary of the rate region satisfies*

$$\tilde{\alpha} = (1 - 2^{-\tilde{R}_B}) \left(1 + \frac{p_S h_{SB} + \sigma_B^2}{\tilde{p}_C h_{CB}} \right) \quad (17)$$

and

$$\tilde{p}_C = \begin{cases} \frac{(p_S h_{SB} + \sigma_B^2)(2^{\tilde{R}_B} - 1)}{h_{CB}}, & F_1 \left(\frac{(p_S h_{SB} + \sigma_B^2)(2^{\tilde{R}_B} - 1)}{h_{CB}} \right) \geq 0, \\ P_C, & F_1(P_C) \leq 0, \\ \hat{p}_C, & \text{otherwise,} \end{cases} \quad (18)$$

where $F_1(x) = 2^{-\tilde{R}_B} h_{CD} h_{CB} \beta x^{1+\lambda} + 2^{-\tilde{R}_B} h_{CD} h_{CB} \sigma_C^2 x - (1 - 2^{-\tilde{R}_B})(p_S h_{SB} + \sigma_B^2) h_{CD} \beta x^\lambda - (1 - 2^{-\tilde{R}_B})(p_S h_{SB} + \sigma_B^2) h_{CD} \sigma_C^2 - p_S h_{SC} \sigma_D^2$, and \hat{p}_C satisfies $F_1(\hat{p}_C) = 0$.

Proof. See Appendix A. □

B. Joint Outage Probability

An outage event occurs when neither the BS nor the DR can decode its desired message correctly. From an information-theoretic viewpoint, when the channel capacity cannot support a target rate, the failure of decoding at the receiver is doomed. Hence, the joint outage probability can be expressed by

$$P_{out} = \mathbb{P}\{R_B < \eta_B, R_D < \eta_D\}, \quad (19)$$

where η_i is the target rate predefined at node $i \in \{B, D\}$ according to a certain QoS requirement. Since the achievable rate is a monotonically increasing function of SINR, (19) can be rewritten as

$$\begin{aligned} P_{out} &= \mathbb{P}\{\gamma_{CB} < \xi_B, \gamma_{CD,C} < \xi_B \cup \min(\gamma_{SC}, \gamma_{CD,S}) < \xi_D\} \\ &= 1 - \mathbb{P}\{\gamma_{CB} \geq \xi_B, \gamma_{SC} \geq \xi_D, \gamma_{CD,C} \geq \xi_B, \gamma_{CD,S} \geq \xi_D\} \end{aligned}$$

where $\xi_i = 2^{\eta_i} - 1$, $i \in \{B, D\}$.

The exact joint outage probability is given in Theorem 2.

Theorem 2. *The joint outage probability of the cellular uplink and the cooperative D2D channel is*

$$P_{out} = \begin{cases} 1, & \alpha \leq \frac{\xi_B}{1+\xi_B}, \\ 1 - (P_1 + P_2)P_3, & \frac{\xi_B}{1+\xi_B} < \alpha \leq 1, \end{cases} \quad (20)$$

where

$$P_1 = \frac{\varphi_{SC}\theta \exp\left[-\frac{\theta}{P_S}\left(\frac{\xi_D(\beta p_C^\lambda + \sigma_C^2)}{\varphi_{SC}\theta} + \frac{1}{\varphi_{SB}}\right)\right]}{\varphi_{SB}\xi_D(\beta p_C^\lambda + \sigma_C^2) + \varphi_{SC}\theta} \exp\left[-\frac{\xi_B(\theta + \sigma_B^2)}{\varphi_{CB}p_C(\alpha - \xi_B + \alpha\xi_B)}\right], \quad (21)$$

$$\begin{aligned} P_2 &= \frac{\varphi_{CB}p_C(\alpha - \xi_B + \alpha\xi_B)}{\varphi_{SB}\xi_B P_S + \varphi_{CB}p_C(\alpha - \xi_B + \alpha\xi_B)} \exp\left[-\frac{\xi_D(\beta p_C^\lambda + \sigma_C^2)}{\varphi_{SC}P_S} - \frac{\xi_B\sigma_B^2}{\varphi_{CB}p_C(\alpha - \xi_B + \alpha\xi_B)}\right] \\ &\times \left(1 - \exp\left[-\frac{\theta}{P_S}\left(\frac{\xi_B P_S}{\varphi_{CB}p_C(\alpha - \xi_B + \alpha\xi_B)} + \frac{1}{\varphi_{SB}}\right)\right]\right), \end{aligned} \quad (22)$$

and

$$P_3 = \begin{cases} \exp\left[-\frac{\xi_B\sigma_D^2}{\varphi_{CD}p_C(\alpha - \xi_B + \alpha\xi_B)}\right], & \frac{\xi_B}{1+\xi_B} < \alpha \leq \frac{\xi_B\xi_D + \xi_B}{\xi_B\xi_D + \xi_B + \xi_D}, \\ \exp\left[-\frac{\xi_D\sigma_D^2}{\varphi_{CD}p_C(1-\alpha)}\right], & \frac{\xi_B\xi_D + \xi_B}{\xi_B\xi_D + \xi_B + \xi_D} < \alpha \leq 1. \end{cases} \quad (23)$$

Proof. See Appendix B. □

Corollary 1. *When p_C approaches infinity, the asymptotic joint outage probability is*

$$\lim_{p_C \rightarrow +\infty} P_{\text{out}} = 1 - \left[1 - \exp\left(-\frac{\theta}{\varphi_{\text{SB}} P_S}\right) \right] \exp\left(-\frac{\xi_D \beta P_C^\lambda}{\varphi_{\text{SC}} P_S}\right). \quad (24)$$

Proof. The proof of Corollary 1 is straightforward, and thus is omitted. \square

Corollary 1 reveals that: (i) the proposed cooperative D2D scheme achieves zero-diversity. On one hand, when $\lambda = 0$, $\lim_{p_C \rightarrow +\infty} P_{\text{out}} = 1 - \left[1 - \exp\left(-\frac{\theta}{\varphi_{\text{SB}} P_S}\right) \right]$; on the other hand, when $\lambda \neq 0$, $\lim_{p_C \rightarrow +\infty} P_{\text{out}} = 1$, which implies that the considered network suffers an outage floor. (ii) the asymptotic outage performance is limited by the first-hop D2D transmission from the DT to the CU, or essentially, the RSI; (iii) the asymptotic joint outage probability is independent of the power splitting factor α , since α does not impact the communication between the DT and the CU.

IV. OPTIMAL POWER ALLOCATION FOR MAXIMIZING THE MINIMUM ACHIEVABLE RATE

In this section, the power allocation scheme (α, p_C) is investigated to optimize the achievable rates, taking consideration of fairness between the cellular uplink and cooperative D2D channels. The max-min criteria [41] is adopted to characterize the fairness, i.e., we try to find the jointly optimal (α, p_C) which maximizes the achievable rate of the bottleneck link. With the knowledge of global CSI, we first formulate the max-min problem. Then we discuss the conditions under which (α, p_C) is optimal. In the end, we prove that the problem of the max-min achievable rate is quasi-concave and provide the optimal solution.

A. Problem Formulation

When global CSI is available at the CU, the maximization problem of the minimum achievable rate for a given power allocation (α, p_C) can be formulated as

$$\begin{aligned} \mathcal{OP}2 : \quad & \max_{\alpha, p_C} R_{\min}(\alpha, p_C) = \min \left(R_B(\alpha, p_C), R_D(\alpha, p_C) \right) \\ & s.t. \quad 0 \leq \alpha \leq 1, \\ & \quad \quad 0 \leq p_C \leq P_C, \end{aligned} \quad (25)$$

where $R_B(\alpha, p_C)$ and $R_D(\alpha, p_C)$ are given in (12) and (13), respectively.

B. Problem Analysis

A key step to solve $\mathcal{OP}2$ is investigating the relation of $R_{SC}(\alpha, p_C)$ and $R_{CD,S}(\alpha, p_C)$ at the optimal power allocation (α^*, p_C^*) , which is provided in the following lemma.

Lemma 2. *The jointly optimal (α^*, p_C^*) satisfies*

$$R_{SC}(\alpha^*, p_C^*) \leq R_{CD,S}(\alpha^*, p_C^*) \quad (26)$$

for $\bar{p}_C < P_C$, and

$$R_{SC}(\alpha^*, p_C^*) \geq R_{CD,S}(\alpha^*, p_C^*) \quad (27)$$

for $\bar{p}_C \geq P_C$, where \bar{p}_C satisfies $F_2(\bar{p}_C) = 0$ and $F_2(x) = h_{CD}\beta x^{1+\lambda} + h_{CD}\sigma_C^2 x - \sigma_D^2 p_S h_{SC}$.

Proof. See Appendix C for the proof of Lemma 1. □

C. Optimal Power Allocation

According to the relation between \bar{p}_C and P_C stated in Lemma 2, the discussion of $\mathcal{OP}2$ can be divided into the following cases.

1) *Case 1:* $\bar{p}_C < P_C$.

Based on Lemma 2, $\mathcal{OP}2$ can be equivalently reformulated as

$$\begin{aligned} \mathcal{OP}2a : \quad & \max_{\alpha, p_C} R_{\min}(\alpha, p_C) = \min(R_B(\alpha, p_C), R_{SC}(p_C)) \\ & s.t. \quad 0 \leq \alpha \leq \bar{\alpha}, \\ & \quad \bar{p}_C \leq p_C \leq P_C, \end{aligned} \quad (28)$$

where $\bar{\alpha} = 1 - \frac{\sigma_D^2 p_S h_{SC}}{(\beta p_C^\lambda + \sigma_C^2) p_C h_{CD}} < 1$, and \bar{p}_C is stated in Lemma 2. The first constraint in $\mathcal{OP}2a$ is directly derived from (26), and the second constraint is obtained from $\bar{\alpha} \geq 0$. Note that $R_{SC}(p_C)$ is independent of α , and then the objective function of $\mathcal{OP}2a$ is a non-decreasing function of α . Without loss of generality, the optimal power splitting factor at the CU can be chosen as $\alpha^* = \bar{\alpha}$. Substituting $\alpha^* = \bar{\alpha}$ into $R_{\min}(\alpha, p_C)$, $\mathcal{OP}2a$ can be simplified as,

$$\begin{aligned} \mathcal{OP}2b : \quad & \max_{p_C} R_{\min}(\bar{\alpha}, p_C) = \min(R_B(\bar{\alpha}, p_C), R_{SC}(p_C)) \\ & s.t. \quad \bar{p}_C \leq p_C \leq P_C, \end{aligned} \quad (29)$$

where $R_B(\bar{\alpha}, p_C)$ is given in (31) on the top of the next page. Obviously, $R_B(\bar{\alpha}, p_C)$ is an increasing function of p_C and $R_{SC}(p_C)$ is a decreasing function of p_C . Therefore, we can prove that $\mathcal{OP}2b$ is quasi-concave with the help of Lemma 1.

$$R_B(\bar{\alpha}, p_C) = \log_2 \left(1 + \frac{h_{CD}h_{CB}p_C(\beta p_C^\lambda + \sigma_C^2) - \sigma_D^2 h_{SC}h_{CB}p_S}{h_{SB}h_{CD}p_S(\beta p_C^\lambda + \sigma_C^2) + \sigma_D^2 h_{SC}h_{CB}p_S} \right) \quad (31)$$

Denote $F_3(x) = R_B(\bar{\alpha}, x) - R_{SC}(x)$. There must exist a \check{p}_C which satisfies $F_3(\check{p}_C) = 0$, and then we have the following discussion on different \check{p}_C .

- If $\check{p}_C < \bar{p}_C$, the minimum achievable rate is limited by $R_{SC}(\bar{\alpha}, p_C)$. The CU should use minimum transmit power to keep the RSI at a low level. Therefore, the optimal transmit power of the CU is $p_C^* = \bar{p}_C$.
- If $\bar{p}_C \leq \check{p}_C \leq P_C$, the minimum achievable rate can be maximized as $R_{\min}^{\max}(\bar{\alpha}, \check{p}_C) = R_B(\bar{\alpha}, \check{p}_C) = R_{SC}(\check{p}_C)$, the optimal transmit power at the CU is $p_C^* = \check{p}_C$.
- If $\check{p}_C > P_C$, the minimum achievable rate is limited by $R_B(\bar{\alpha}, p_C)$. The CU will transmit with the maximum power to improve the achievable rate of the cellular uplink, i.e., $p_C^* = P_C$.

After p_C^* is obtained, we have the optimal power splitting factor as

$$\alpha^* = 1 - \frac{\sigma_D^2 p_S h_{SC}}{[\beta(p_C^*)^\lambda + \sigma_C^2] p_C^* h_{CD}}. \quad (32)$$

2) *Case 2: $\bar{p}_C \geq P_C$.*

In this case, $\mathcal{OP}2$ can be reformulated as

$$\begin{aligned} \mathcal{OP}2c: \quad & \max_{\alpha, p_C} R_{\min}(\alpha, p_C) = \min(R_B(\alpha, p_C), R_{CD,S}(\alpha, p_C)) \\ & s.t. \quad 0 \leq \alpha \leq 1, \\ & \quad \quad 0 \leq p_C \leq P_C. \end{aligned} \quad (33)$$

The objective function in $\mathcal{OP}2c$ is a non-decreasing function of p_C , therefore the optimal transmit power at the CU can be selected as $p_C^* = P_C$. Now $\mathcal{OP}2c$ is simplified as

$$\begin{aligned} \mathcal{OP}2d: \quad & \max_{\alpha, p_C} R_{\min}(\alpha, P_C) = \min(R_B(\alpha, P_C), R_{CD,S}(\alpha, P_C)) \\ & s.t. \quad 0 \leq \alpha \leq 1. \end{aligned} \quad (34)$$

Similar to the discussion of $\mathcal{OP}2b$, we have that $R_B(\alpha, P_C)$ and $R_{CD,S}(\alpha, P_C)$ are monotonically increasing and decreasing function of α . By applying Lemma 1 again, we know that $\mathcal{OP}2d$ is also quasi-concave with respect to α . Denote $F_4(x) = R_B(x, P_C) - R_{CD,S}(x, P_C)$, and it is easy to verify that $F_4(0) < 0$ and $F_4(1) > 0$. There must exist $\check{\alpha}$ which satisfies $F_4(\check{\alpha}) = 0$,

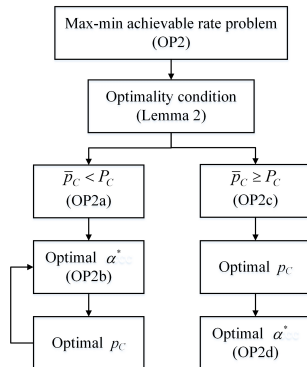


Fig. 2: Procedure to solve the max-min achievable rate problem.

such that the minimum achievable rate can be maximized as $R_{\min}^{\max}(\check{\alpha}, P_C) = R_B(\check{\alpha}, P_C) = R_{CD,S}(\check{\alpha}, P_C)$. Therefore the optimal power splitting factor in this case is $\alpha^* = \check{\alpha}$.

D. Summary

As a summary of Case 1 and Case 2, we organize the procedure to solve the max-min achievable rate problem in Fig. 2, and propose an algorithm (denoted as Algorithm 1) to compute the jointly optimal (α, p_C) . The idea of Algorithm 1 is sequentially identifying and maximize the bottleneck link of the considered network to meet the max-min criteria. The pseudocode of Algorithm 1 is given on the top of the next page.

V. OPTIMAL POWER ALLOCATION FOR MINIMIZING THE JOINT OUTAGE PROBABILITY

When only statistical CSI is available, the CU cannot adjust transmit power or power splitting factor to maximize the achievable rate. Instead, in this paper, we consider that the CU optimizes the power allocation scheme (α, p_C) to improve the outage performance. The joint outage probability minimization problem can be formulated as

$$\begin{aligned}
 \mathcal{OP3}: \quad & \min_{\alpha, p_C} P_{\text{out}}(\alpha, p_C) \\
 & s.t. \quad \frac{\xi_B}{1 + \xi_B} < \alpha \leq 1, \\
 & \quad \quad 0 \leq p_C \leq P_C,
 \end{aligned} \tag{35}$$

where $P_{\text{out}}(\alpha, p_C)$ is given in Theorem 2. Note that $P_{\text{out}}(\alpha, p_C)$ is a combination of exponential functions and rational fractions, which is hardly tractable. As an alternative, we will derive the

Algorithm 1 Algorithm to compute the optimal power allocation of the max-min achievable rate problem

Require: Global CSI ($h_{SB}, h_{CB}, h_{SC}, h_{CD}$); average noise power ($\sigma_B^2, \sigma_C^2, \sigma_D^2$); SIS parameters (β, λ); power constraint at the CU (P_C);

Ensure: Optimal power allocation (α, p_C);

- 1: Solve $F_2(\bar{p}_C) = 0$ to get \bar{p}_C ;
 - 2: **if** $\bar{p}_C < P_C$ **then**
 - 3: Solve $F_3(x) = 0$ to get \check{p}_C ;
 - 4: **if** $\check{p}_C < \bar{p}_C$ **then**
 - 5: $p_C^* = \bar{p}_C$;
 - 6: **else if** $\check{p}_C > P_C$ **then**
 - 7: $p_C^* = P_C$;
 - 8: **else**
 - 9: $p_C^* = \check{p}_C$;
 - 10: **end if**
 - 11: $\alpha^* = 1 - \frac{\sigma_D^2 p_S h_{SC}}{[\beta(p_C^*)^\lambda + \sigma_C^2] p_C^* h_{CD}}$;
 - 12: **else**
 - 13: $p_C^* = P_C$;
 - 14: Solve $F_4(\alpha^*) = 0$ to get α^* ;
 - 15: **end if**
-

upper bound of $P_{\text{out}}(\alpha, p_C)$ and loosen $\mathcal{OP}3$ to obtain a suboptimal power allocation scheme $(\alpha^{\otimes}, p_C^{\otimes})$.

A. Upper Bound of the Joint Outage Probability

We use the worst-case interference approximation to obtain the upper bound of $P_{\text{out}}(\alpha, p_C)$. Considering that the interference caused by D2D transmission at the BS cannot exceed the threshold θ , the SINR at the BS has a lower bound of $\gamma_{CB} \geq \frac{\alpha p_C h_{CB}}{\theta + (1-\alpha)p_C h_{CB} + \sigma_B^2}$. Following the similar approach in Appendix B, the upper bound of $P_{\text{out}}(\alpha, p_C)$ for $\frac{\xi_B}{1+\xi_B} < \alpha \leq 1$ can be calculated as

$$P_{\text{out}} \leq 1 - (P_1 + \tilde{P}_2) P_3 = \tilde{P}_{\text{out}}, \quad (36)$$

where \tilde{P}_2 is given in (37). P_1 and P_3 are given in (21) and (23), respectively.

$$\tilde{P}_2 = \exp \left[-\frac{\xi_D \beta (p_C^\lambda + \sigma_C^2)}{\varphi_{SC} P_S} - \frac{\xi_B (\theta + \sigma_B^2)}{\varphi_{CB} p_C (\alpha - \xi_B + \alpha \xi_B)} \right] \times \left[1 - \exp \left(-\frac{\theta}{\varphi_{SB} P_S} \right) \right], \quad (37)$$

The upper bound in (36) provides a more tractable expression. In addition, as will be shown in Section VI, the derived upper bound offers a good approximation when the interference threshold θ is much smaller than the maximum transmit power at the DT, i.e., $\frac{\theta}{P_S} \rightarrow 0$. Therefore, $\mathcal{OP}3$ can be relaxed as

$$\begin{aligned} \mathcal{OP}3a : \quad & \min_{\alpha, p_C} \tilde{P}_{out}(\alpha, p_C) \\ & s.t. \quad \frac{\xi_B}{1 + \xi_B} < \alpha \leq 1, \\ & \quad \quad 0 \leq p_C \leq P_C. \end{aligned} \quad (38)$$

In general, the objective function of $\mathcal{OP}3a$ is not jointly concave of (α, p_C) . However, as shown in the following, $\mathcal{OP}3a$ is quasi-concave.

B. Optimization of the Power Splitting Factor

We first analyze the optimal power splitting factor α^* for a fixed p_C . In order to predigest the analysis, we introduce the following variables and functions for notation convenience,

$$P_1 = A \times f(\alpha), \quad \tilde{P}_2 = B \times f(\alpha), \quad P_3 = g(\alpha)$$

where

$$\begin{aligned} A &= \frac{\varphi_{SC} \theta \exp \left[-\frac{\theta}{P_S} \left(\frac{\xi_D (\beta p_C^\lambda + \sigma_C^2)}{\varphi_{SC} \theta} + \frac{1}{\varphi_{SB}} \right) \right]}{\varphi_{SB} \xi_D (\beta p_C^\lambda + \sigma_C^2) + \varphi_{SC} \theta}, \\ B &= \exp \left(-\frac{\xi_D (\beta p_C^\lambda + \sigma_C^2)}{\varphi_{SC} P_S} \right) \times \left[1 - \exp \left(-\frac{\theta}{\varphi_{SB} P_S} \right) \right], \\ f(\alpha) &= \exp \left[-\frac{\xi_B (\theta + \sigma_B^2)}{\varphi_{CB} p_C (\alpha - \xi_B + \alpha \xi_B)} \right], \end{aligned}$$

and $g(\alpha)$ is given in (23).

By (36), the upper bound of joint outage probability can be rewritten as

$$\tilde{P}_{out}(\alpha) = 1 - (A + B) f(\alpha) g(\alpha). \quad (39)$$

Taking the derivative of $\tilde{P}_{out}(\alpha)$, we have

$$\begin{aligned} \frac{\partial}{\partial \alpha} \tilde{P}_{out}(\alpha) &= -(A+B) \left[g(\alpha) \frac{\partial}{\partial \alpha} f(\alpha) + f(\alpha) \frac{\partial}{\partial \alpha} g(\alpha) \right]. \end{aligned} \quad (40)$$

Furthermore, we have

$$\begin{aligned} \frac{\partial}{\partial \alpha} f(\alpha) &= \frac{\varphi_{CBPC}(1+\xi_B)\xi_B(\theta+\sigma_B^2)}{\underbrace{[\varphi_{CBPC}(1+\xi_B)\alpha - \varphi_{CBPC}\xi_B]^2}_{\triangleq h(\alpha)}} f(\alpha) \\ &= h(\alpha) f(\alpha), \end{aligned} \quad (41)$$

and

$$\frac{\partial}{\partial \alpha} g(\alpha) = l(\alpha) g(\alpha), \quad (42)$$

where

$$l(\alpha) = \begin{cases} \frac{\xi_B(1+\xi_B)\sigma_D^2}{\varphi_{CDPC}(\alpha-\xi_B+\alpha\xi_B)^2}, & \frac{\xi_B}{1+\xi_B} < \alpha \leq \frac{\xi_B\xi_D+\xi_B}{\xi_B\xi_D+\xi_B+\xi_D}, \\ -\frac{\xi_D\sigma_D^2}{\varphi_{CDPC}(1-\alpha)^2}, & \frac{\xi_B\xi_D+\xi_B}{\xi_B\xi_D+\xi_B+\xi_D} < \alpha \leq 1. \end{cases} \quad (43)$$

Then (40) can be rewritten as

$$\frac{\partial}{\partial \alpha} \tilde{P}_{out}(\alpha) = -(A+B) f(\alpha) g(\alpha) [h(\alpha) + l(\alpha)]. \quad (44)$$

For $\frac{\xi_B}{1+\xi_B} < \alpha \leq \frac{\xi_B\xi_D+\xi_B}{\xi_B\xi_D+\xi_B+\xi_D}$, we have $\frac{\partial}{\partial \alpha} \tilde{P}_{out}(\alpha) < 0$, i.e., $\tilde{P}_{out}(\alpha, p_C)$ is a monotonically decreasing function in $\left(\frac{\xi_B}{1+\xi_B}, \frac{\xi_B\xi_D+\xi_B}{\xi_B\xi_D+\xi_B+\xi_D}\right]$. In this case, the optimal α is

$$\alpha^{\otimes} = \frac{\xi_B\xi_D + \xi_B}{\xi_B\xi_D + \xi_B + \xi_D}. \quad (45)$$

For $\frac{\xi_B\xi_D+\xi_B}{\xi_B\xi_D+\xi_B+\xi_D} < \alpha \leq 1$, let $\frac{\partial}{\partial \alpha} \tilde{P}_{out}(\alpha) = 0$, which is equivalent to $h(\alpha) + l(\alpha) = 0$. It is easy to verify that equation $h(\alpha) + l(\alpha) = 0$ has a sole positive root which is the optimal α ,

$$\alpha^{\otimes} = \frac{K+M}{1+M} \quad (46)$$

where $K = \frac{\xi_B}{1+\xi_B}$, $M = \sqrt{\frac{\varphi_{CD}(\theta+\sigma_B^2)K}{\varphi_{CB}\xi_D\sigma_D^2}}$. Since $0 < K < 1$, we have $K < \frac{K+M}{1+M} < 1$, i.e., $\alpha = \frac{K+M}{1+M}$ is a feasible solution to $\mathcal{OP}3a$.

C. Optimization of Transmit Power at the CU

Substituting α^{\circledast} into (36), $\tilde{P}_{out}(\alpha^{\circledast}, p_C)$ can be treated as a function only depending on p_C ,

$$\tilde{P}_{out}(\alpha^{\circledast}, p_C) = 1 - j(p_C) k(p_C) \quad (47)$$

where

$$\begin{aligned} j(p_C) &= \frac{E}{Cp_C^\lambda + D} + F, \quad k(p_C) = \exp\left(-\frac{Gp_C^{1+\lambda} + H}{p_C} + I\right), \\ C &= \varphi_{SB}\xi_D\beta, \quad D = \varphi_{SB}\xi_D\sigma_C^2 + \varphi_{SC}\theta, \\ E &= \varphi_{SC}\theta \exp\left(\frac{-\theta}{\varphi_{SB}P_S}\right), \quad F = 1 - \exp\left(\frac{-\theta}{\varphi_{SB}P_S}\right), \quad G = \frac{\xi_D\beta}{\varphi_{SC}P_S}, \\ H &= \frac{\xi_B(\theta + \sigma_B^2)}{\varphi_{CB}(\alpha^{\circledast} - \xi_B + \alpha^{\circledast}\xi_B)} + \frac{\xi_D\sigma_D^2}{\varphi_{CD}(1 - \alpha^{\circledast})}, \quad I = \frac{\xi_D\sigma_C^2}{\varphi_{SC}P_S} \end{aligned}$$

Let $\partial\tilde{P}_{out}/\partial\alpha = 0$, we have the following equation,

$$\begin{aligned} &\lambda C^2 F G p_C^{1+3\lambda} + \lambda C (2DF + E) G p_C^{1+2\lambda} \\ &+ \lambda (D^2 F G + DEG + CE) p_C^{1+\lambda} - C^2 F H p_C^{2\lambda} \\ &- C (2DF + E) H p_C^\lambda - D (DF + E) H = 0. \end{aligned} \quad (48)$$

Denote the generalized polynomial [42] on the left hand side of (48) by $Q(p_C)$. It is easy to see that $Q(p_C)$ has only one sign change between the third and fourth terms. According to the *Descartes' Rule of Signs* [43], the equation $Q(p_C) = 0$ has at most one positive root. Let p_C° be the positive root of $Q(p_C) = 0$, then we have the following discussions.

- Assume $p_C^\circ \in \emptyset$. Since $Q(0) = -D(DF + E)H < 0$, we know $\frac{\partial}{\partial p_C}\tilde{P}_{out}\Big|_{p_C=0} < 0$ for $p_C \geq 0$. Therefore, \tilde{P}_{out} is a monotonically decreasing function of p_C . The optimal transmit power at the CU is

$$p_C^{\circledast} = P_C. \quad (49)$$

- If $p_C^\circ \notin \emptyset$ and $p_C^\circ \notin [0, P_C]$, \tilde{P}_{out} is a decreasing function of p_C in the feasible region of $\mathcal{OP}3a$. In this case, the optimal solution is $p_C^{\circledast} = P_C$.
- If $p_C^\circ \notin \emptyset$ and $p_C^\circ \in [0, P_C]$, then \tilde{P}_{out} is a decreasing function of p_C for $0 \leq p_C \leq p_C^\circ$ and an increasing function for $p_C^\circ \leq p_C \leq P_C$. Hence, the optimal transmit power at the CU is

$$p_C^{\circledast} = p_C^\circ. \quad (50)$$

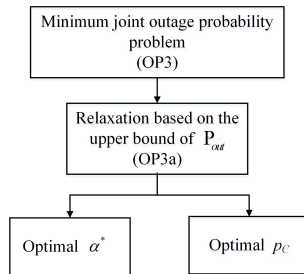


Fig. 3: Procedure to solve the minimum joint outage probability problem.

D. Summary

Following the analyses in Section V-B and V-C, the suboptimal solution to $\mathcal{OP3}$ can be summarized as

$$(\alpha^{\otimes}, p_C^{\otimes}) = \left(\max \left(\frac{\xi_B \xi_D + \xi_B}{\xi_B \xi_D + \xi_B + \xi_D}, \frac{K + M}{1 + M} \right), \min(p_C^{\circ}, P_C) \right). \quad (51)$$

The procedure to solve the minimum joint outage probability problem is illustrated in Fig. 3. Apparently, the optimal power splitting factor is independent of the transmit power at the CU, therefore α^{\otimes} and p_C^{\otimes} can be individually obtained.

VI. NUMERICAL RESULTS

In this section, we use numerical simulations to verify the performance analysis and evaluate the proposed power allocation algorithms. The channel coefficient is independently realized in each simulation according to the Gaussian distribution. The main simulation parameters are listed in Table I, other involved parameters will be stated in each simulation. In addition, all non-linear equations are solved with the bisection method [44].

Fig. 4 shows the achievable rate region of the proposed cooperative D2D network with different λ , which is the SIS parameter defined in (2). We can see that with the decrease of λ , the proposed network has a larger achievable rate region. The maximum achievable rate of the cellular uplink for different λ is the same, since the uplink rate is not affected by RSI. However, the maximum achievable rate of the cooperative D2D link decrease as λ grows due to the strengthened RSI. At point **A** for $\lambda = 0$ or **B** for $\lambda = 0.5$, the first and second hop of the cooperative D2D link achieves the identical rate. Further increase of R_B requires larger p_C or α , which will cause rapid descent of R_D .

TABLE I: Main Simulation Parameters

Parameters	Value
Carrier center frequency	2GHz
Channel bandwidth	180kHz
Peak transmit power of the users	23dBm
Receiver noise density	-174dBm
Cell radius	200m
Distance between the DT and the DR	150-300m
Minimum distance between the users and the BS	30m
Decay factor of the path-loss	3.8

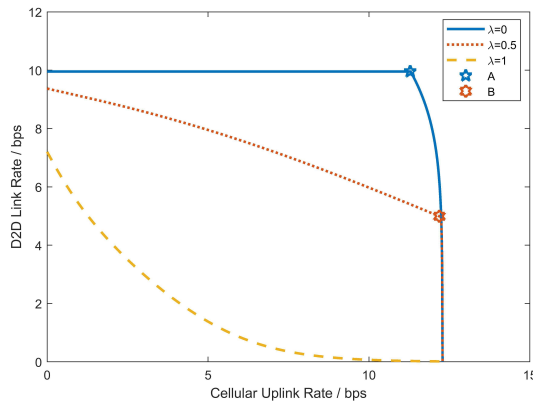


Fig. 4: Achievable rate region ($h_{SB} = h_{SC} = h_{CB} = h_{CD} = 0.5$, $\beta = 1$, $P_S = 23\text{dBm}$, $P_C = 23\text{dBm}$).

Fig. 5 shows the joint outage probability of the considered system with a fixed power splitting factor at the CU. On one hand, we observe that the curves of theoretical analysis perfectly match the curves of Monte Carlo simulation results, which confirms our analytical results in Section III. On the other hand, the curves of the upper bound of the joint outage probability almost overlap the curves of the exact joint outage probability, which indicates that the upper bound shown in (36) can be regarded as an accurate approximation of the exact joint outage probability.

Roughly speaking, the curve of the joint outage probability is a “V” shape. With the increase of p_C , the joint outage probability first decreases due to the improvement of SINR/SNR. However, a further increase of p_C causes more severe RSI at the CU, and then leads to the growth of joint outage probability, since the joint outage probability is dominated by the link between the DT

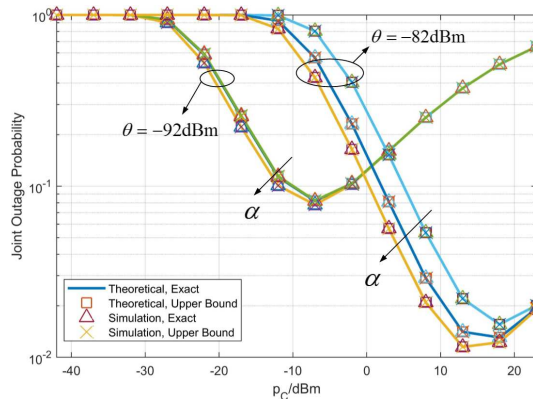


Fig. 5: Joint outage probability versus p_C ($\alpha = [0.6, 0.7, 0.8]$, $\lambda = 0.1$, $\beta = 1$, $P_S = 23\text{dBm}$, $\eta_B = \eta_D = 1$).

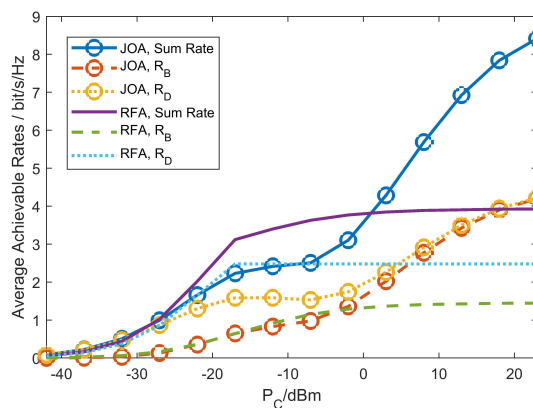


Fig. 6: Comparison of average achievable rate with difference power allocation algorithms ($\theta = -92\text{dBm}$, $\lambda = 0.1$, $\beta = 1$, $P_S = 23\text{dBm}$, $\eta_B = \eta_D = 1$).

and the CU in the high transmit power region. Furthermore, the curves of joint outage probability with different α converges when p_C is high enough. This can be explained by asymptotic analysis of P_{out} in Section III. For fixed and relatively smaller p_C , the joint outage probability decreases with α , since the joint outage probability is limited by the cellular uplink transmission from the CU to the BS. Besides, a larger θ will loosen the transmit power constraint at the D2D transmitter and leads to a lower minimum joint outage probability at the cost of higher transmit power of the CU.

Fig. 6 illustrates the average achievable rate with the proposed joint optimization algorithm (JOA). For comparison, we adopt the random- α fixed- p_C algorithm (RFA) as a benchmark,

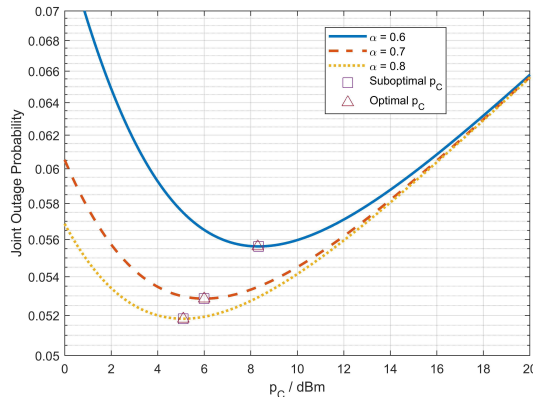


Fig. 7: Joint outage probability with different α ($\theta = -92$ dBm, $\lambda = 0.1$, $\beta = 1$, $P_S = 23$ dBm, $\eta_B = \eta_D = 1$).

where the CU uniformly selects α from $[0, 1]$ and transmits with the maximum power. From a sum rate viewpoint, the RFA outperforms the JOA when $P_C < 0$ dBm. When $P_C > 0$ dBm, the RFA introduces severe self-interference due to maximum transmit power at the CU. Meanwhile, the randomly chosen α restricts the achievable rate at the BS. Therefore, the sum rates of RFA reaches a plateau rapidly and results in the waste of transmit power at the CU. With the JOA, the CU can dynamically maximize the achievable rate of the bottleneck link according to p_C . From the decoding order at the BS and the DUE receiver, we know that the considered system is limited by the cellular uplink channel capacity. As shown in Fig. 6, R_B with JOA grows monotonically as P_C increases. For $P_C > 10$ dBm, R_B and R_D converge to a same value, which confirms the validity of the proposed JOA. In addition, the JOA achieves a much higher sum rate than the RFA does, which demonstrates that the transmit power at the CU can be more effectively utilized with JOA.

Fig. 7 and Fig. 8 provide the simulation results of the suboptimal power allocation in the sense of joint outage probability minimization. The optimal solutions are carried out by exhaustive search. It can be observed that for fixed α or p_C , the suboptimal solutions is very close to the optimal solutions. As analyzed in Section V, α and p_C can be optimized separately, and therefore the effectiveness of the proposed suboptimal power allocation is verified.

In order to investigate the relation between the network performance and the performance of SIS, we also simulate the joint outage probability as a function of λ , with different β . The HD system is adopted as a benchmark. We can see that if the TRR is high enough, the FD

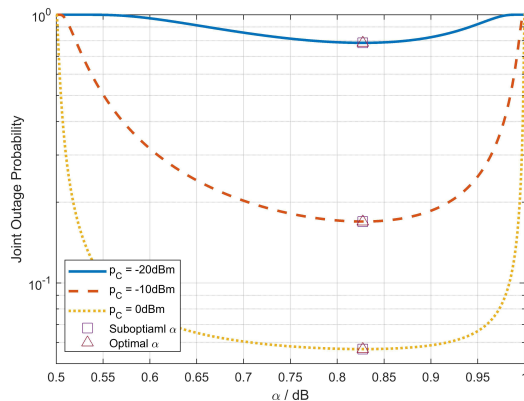


Fig. 8: Joint outage probability with different p_C ($\theta = -92\text{dBm}$, $\lambda = 0.1$, $\beta = 1$, $P_S = 23\text{dBm}$, $\eta_B = \eta_D = 1$).

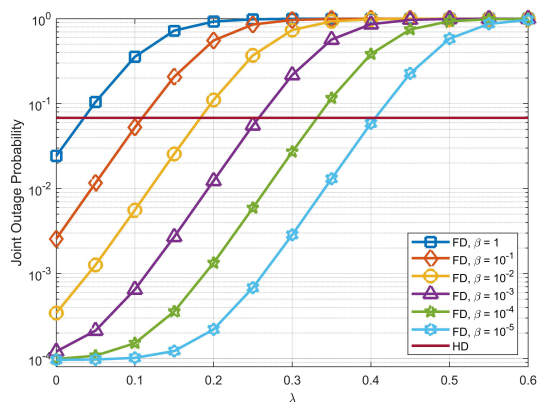


Fig. 9: Joint outage probability versus λ ($\theta = -92\text{dBm}$, $\alpha = 0.95$, $p_C = 23\text{dBm}$, $P_S = 23\text{dBm}$, $\eta_B = \eta_D = 1$).

network outperforms the HD counterpart. By (3), the TRR at each cross point where the FD and HD networks achieve the same outage performance is 130dB. In other words, the advantage of the FD mode over the HD mode lies on the TRR rather than the unilateral value of λ and β . However, different λ and β provide distinct tradeoff between the outage performance of the cellular uplink and the cooperative D2D link. In Fig. 10, we present the outage probability for the cellular uplink and the cooperative D2D link with TRR fixed to 130dB. We can see that the outage probability of the cellular uplink decreases with λ , and the outage probability of the cooperative D2D link increases as $\lambda \rightarrow 1$. For $\beta = 10^{-2}$ and $\beta = 10^{-4}$, two reverse points at $\lambda = 0.2$ and $\lambda = 0.8$ are observed. This phenomenon can be explained by investigating the

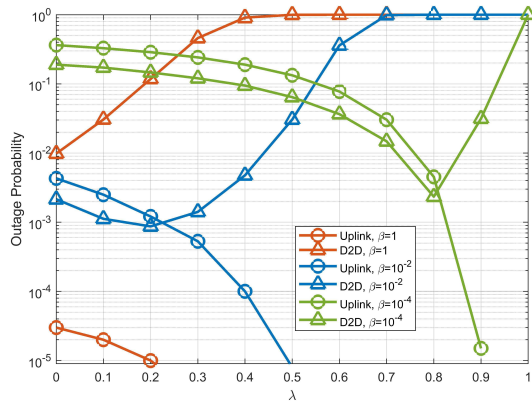


Fig. 10: Joint outage probability versus λ ($\theta = -92\text{dBm}$, $\alpha = 0.95$, $p_C = 23\text{dBm}$, $P_S = 23\text{dBm}$, $\eta_B = \eta_D = 1$).

relation among the TRR, p_C , λ and β . For fixed β and TRR, we have $p_C = \sqrt[1-\lambda]{TRR \times \beta}$, which indicates that p_C is an increasing function of λ . Note that $R_B(\alpha, p_C)$ is also an increasing function of λ , and therefore the outage probability of the cellular uplink monotonically decreases with λ . However, with the increase of p_C , the outage probability of the first-hop D2D link from the DT to the CU is worsen due to strengthened RSI, meanwhile the outage probability of the second-hop D2D link from the CU to the DR is improved due to elevated SNR. In addition, the outage probabilities of the cellular uplink and the cooperative D2D link are close when $\lambda \rightarrow 0$, but diverge when $\lambda \rightarrow 1$, which implies that smaller λ provides better fairness between the cellular uplink and the cooperative D2D link.

VII. CONCLUSION

In this paper, we proposed a cooperative underlay D2D network, where the cellular user is assigned as an FD relay with superposition coding and the D2D receiver performs successive interference cancellation to decode the desired signal. Both achievable rate region and joint outage probability were analyzed. To optimize the network performance, two power allocation schemes were proposed in the sense of max-min achievable rate and minimizing the upper bound of the joint outage probability. The correctness of theoretical analysis and the validity of power allocation schemes have been verified by numerical simulations, which reveals the superiority of the proposed FD cooperative D2D network.

APPENDIX A
PROOF OF THEOREM 1

By the first constraint in (16), we can express α as a function of p_C ,

$$\alpha = (1 - 2^{-\tilde{R}_B}) \left(1 + \frac{p_S h_{SB} + \sigma_B^2}{p_C h_{CB}} \right). \quad (52)$$

Then, $R_{CD,S}(\alpha, p_C)$ can be rewritten as (53)

$$R_{CD,S}(p_C) = \log_2 \left(1 - \frac{h_{CD}(p_S h_{SB} + \sigma_B^2)(1 - 2^{-\tilde{R}_B})}{h_{CB}\sigma_D^2} + \frac{h_{CD}2^{-\tilde{R}_B}}{\sigma_D^2} p_C \right). \quad (53)$$

Since $0 \leq \alpha \leq 1$, we have

$$p_C \geq \frac{(p_S h_{SB} + \sigma_B^2)(2^{\tilde{R}_B} - 1)}{h_{CB}}. \quad (54)$$

In addition, $\frac{(p_S h_{SB} + \sigma_B^2)(2^{\tilde{R}_B} - 1)}{h_{CB}} \leq P_C$ is guaranteed by $\tilde{R}_B \leq R_B^{\max}$. Therefore we can reformulate $\mathcal{OP}1$ as follows,

$$\begin{aligned} & \max_{\alpha, p_C} \min(R_{SC}(p_C), R_{CD,S}(p_C)) \\ & \text{s.t. } \frac{(p_S h_{SB} + \sigma_B^2)(2^{\tilde{R}_B} - 1)}{h_{CB}} \leq p_C \leq P_C. \end{aligned} \quad (55)$$

Obviously, $R_{CD,S}(p_C)$ is a monotonically increasing function of p_C , and $R_{SC}(p_C)$ is a monotonically decreasing function of p_C . By Lemma 1, the optimization problem in (55) is quasi-concave.

Denote $F_1(x) = R_{CD,S}(x) - R_{SC}(x)$, then the solution to (55) can be divided in three cases:

Case 1: $F_1\left(\frac{(p_S h_{SB} + \sigma_B^2)(2^{\tilde{R}_B} - 1)}{h_{CB}}\right) \geq 0$. In this case, the cooperative D2D link is restricted by the first-hop from the DT to the CU. The CU has to limit the transmit power to avoid severe RSI. Therefore p_C is chosen to meet the lower bound as $p_C = \frac{(p_S h_{SB} + \sigma_B^2)(2^{\tilde{R}_B} - 1)}{h_{CB}}$.

Case 2: $F_1(P_C) \leq 0$. In this case, the bottleneck link in the cooperative D2D channel is the second-hop from the CU to the DT. Therefore the CU uses the highest transmit power to achieve the Pareto boundary, i.e., $p_C = P_C$.

Case 3: $F_1\left(\frac{(p_S h_{SB} + \sigma_B^2)(2^{\tilde{R}_B} - 1)}{h_{CB}}\right) < 0$ and $F_1(P_C) > 0$. In this case, there must exist a \hat{p}_C such that the achievable rate of the cooperative D2D channel can be maximized as $R_D^{\max} = R_{CD,S}(\hat{p}_C) = R_{SC}(\hat{p}_C)$. The uniqueness of \hat{p}_C is guaranteed by the monotonicity of $R_{SC}(p_C)$ and $R_{CD,S}(p_C)$.

Substituting the p_C in Cases 1-3 into (52), the proof of Theorem 1 is completed.

APPENDIX B
PROOF OF THEOREM 2

Conditioning on α , the discussion of P_{out} can be divided into the following two cases.

Case A: $\alpha \leq \frac{\xi_B}{1+\xi_B}$. In this case, we have $\frac{\alpha}{1-\alpha} \leq \xi_B$. On one hand, we know that $\gamma_{CD,C} < \frac{\alpha}{1-\alpha} \leq \xi_B$, the DR will fail to decode x_C , and thus cannot perform SIC to further decode x_S . On the other hand, we have $\gamma_{CB} < \frac{\alpha}{1-\alpha} \leq \xi_B$, which suggests that the decoding at the BS also fails. Therefore, the joint outage probability $P_{out} = 1$.

Case B: $\alpha > \frac{\xi_B}{1+\xi_B}$. Considering that $\gamma_{CD,C}$ and $\gamma_{CD,S}$ are independent of γ_{CB} and γ_{SC} , P_{out} can be rewritten as

$$\begin{aligned}
P_{out} &= 1 - \mathbb{P}\{\gamma_{CB} \geq \xi_B, \gamma_{SC} \geq \xi_D\} \\
&\quad \times \mathbb{P}\{\gamma_{CD,C} \geq \xi_B, \gamma_{CD,S} \geq \xi_D\} \\
&= 1 - \mathbb{E}_{h_{SB}}[\mathbb{P}\{\gamma_{CB} \geq \xi_B, \gamma_{SC} \geq \xi_D | h_{SB}\}] \\
&\quad \times \mathbb{P}\{\gamma_{CD,C} \geq \xi_B, \gamma_{CD,S} \geq \xi_D\} \\
&= 1 - \left(\underbrace{\mathbb{P}\{\gamma_{CB} \geq \xi_B, \gamma_{SC} \geq \xi_D, h_{SB} \geq \frac{\theta}{P_S}\}}_{\triangleq P_1} \right. \\
&\quad \left. + \underbrace{\mathbb{P}\{\gamma_{CB} \geq \xi_B, \gamma_{SC} \geq \xi_D, h_{SB} < \frac{\theta}{P_S}\}}_{\triangleq P_2} \right) \\
&\quad \times \underbrace{\mathbb{P}\{\gamma_{CD,C} \geq \xi_B, \gamma_{CD,S} \geq \xi_D\}}_{\triangleq P_3}. \tag{56}
\end{aligned}$$

P_1 can be further expanded as

$$P_1 = \underbrace{\mathbb{P}\{\gamma_{CB} \geq \xi_B\}}_{Q_1} \underbrace{\mathbb{P}\{\gamma_{SC} \geq \xi_D | h_{SB} \geq \frac{\theta}{P_S}\} \mathbb{P}\{h_{SB} \geq \frac{\theta}{P_S}\}}_{Q_2}. \tag{57}$$

Following the Rayleigh fading assumption, we have the probability density function (pdf) of h_{ij} as $f_{h_{ij}}(x) = \frac{1}{\varphi_{ij}} e^{-\frac{x}{\varphi_{ij}}}$, and thus Q_1 can be trivially obtained as

$$\begin{aligned}
Q_1 &= \mathbb{P}\left\{ h_{CB} \geq \frac{\xi_B(\theta + \sigma_B^2)}{p_C(\alpha - \xi_B + \alpha\xi_B)} \right\} \\
&= \int_{\frac{\xi_B(\theta + \sigma_B^2)}{p_C(\alpha - \xi_B + \alpha\xi_B)} }^{+\infty} \frac{1}{\varphi_{CB}} e^{-\frac{h_{CB}}{\varphi_{CB}}} dh_{CB} \\
&= \exp\left[-\frac{\xi_B(\theta + \sigma_B^2)}{\varphi_{CB} p_C(\alpha - \xi_B + \alpha\xi_B)} \right]. \tag{58}
\end{aligned}$$

And Q_2 can be calculated as

$$\begin{aligned}
Q_2 &= \mathbb{P}\left\{h_{SC} \geq \frac{\xi_D h_{SB}(\beta p_C^\lambda + \sigma_C^2)}{\theta} \mid h_{SB} \geq \frac{\theta}{P_S}\right\} \mathbb{P}\{h_{SB} \geq \frac{\theta}{P_S}\} \\
&= \int_{\frac{\theta}{P_S}}^{+\infty} \frac{1}{\varphi_{SB}} \exp\left[-\frac{\xi_D h_{SB}(\beta p_C^\lambda + \sigma_C^2)}{\varphi_{SC}\theta}\right] \exp\left(-\frac{h_{SB}}{\varphi_{SB}}\right) dh_{SB} \\
&= \frac{\varphi_{SC}\theta \exp\left[-\frac{\theta}{P_S}\left(\frac{\xi_D(\beta p_C^\lambda + \sigma_C^2)}{\varphi_{SC}\theta} + \frac{1}{\varphi_{SB}}\right)\right]}{\varphi_{SB}\xi_D(\beta p_C^\lambda + \sigma_C^2) + \varphi_{SC}\theta}.
\end{aligned} \tag{59}$$

Substituting (58) and (59) back into (57), we have P_1 in (21).

Similarly, P_2 can be expanded as

$$P_2 = \underbrace{\mathbb{P}\{\gamma_{SC} \geq \xi_D\}}_{Q_3} \underbrace{\mathbb{P}\{\gamma_{CB} \geq \xi_B \mid h_{SB} < \frac{\theta}{P_S}\}}_{Q_4} \mathbb{P}\{h_{SB} < \frac{\theta}{P_S}\}. \tag{60}$$

Q_3 can be computed as

$$\begin{aligned}
Q_3 &= \mathbb{P}\left\{h_{SC} \geq \frac{\xi_D(\beta p_C^\lambda + \sigma_C^2)}{P_S}\right\} \\
&= \int_{\frac{\xi_D(\beta p_C^\lambda + \sigma_C^2)}{P_S}}^{+\infty} \frac{1}{\varphi_{SC}} e^{-\frac{h_{SC}}{\varphi_{SC}}} dh_{SC} \\
&= \exp\left[-\frac{\xi_D(\beta p_C^\lambda + \sigma_C^2)}{\varphi_{SC}P_S}\right].
\end{aligned} \tag{61}$$

Q_4 can be calculated as

$$\begin{aligned}
Q_4 &= \mathbb{P}\left\{h_{CB} \geq \frac{\xi_B(P_S h_{SB} + \sigma_B^2)}{p_C(\alpha - \xi_B + \alpha\xi_B)} \mid h_{SB} < \frac{\theta}{P_S}\right\} \mathbb{P}\{h_{SB} < \frac{\theta}{P_S}\} \\
&= \int_0^{\frac{\theta}{P_S}} \frac{1}{\varphi_{SB}} \exp\left[-\frac{\xi_B(P_S h_{SB} + \sigma_B^2)}{p_C(\alpha - \xi_B + \alpha\xi_B)}\right] \exp\left(-\frac{h_{SB}}{\varphi_{SB}}\right) dh_{SB} \\
&= \frac{\varphi_{CB} p_C(\alpha - \xi_B + \alpha\xi_B)}{\varphi_{SB}\xi_B P_S + \varphi_{CB} p_C(\alpha - \xi_B + \alpha\xi_B)} \\
&\quad \times \exp\left[-\frac{\xi_B \sigma_B^2}{\varphi_{CB} p_C(\alpha - \xi_B + \alpha\xi_B)}\right] \\
&\quad \times \left(1 - \exp\left[-\frac{\theta}{P_S}\left(\frac{\xi_B P_S}{\varphi_{CB} p_C(\alpha - \xi_B + \alpha\xi_B)} + \frac{1}{\varphi_{SB}}\right)\right]\right).
\end{aligned} \tag{62}$$

Substituting (61) and (62) back into (60), we have P_2 in (22).

P_3 can be rewritten as

$$P_3 = \mathbb{P}\{h_{CD} \geq \frac{\xi_B \sigma_D^2}{p_C(\alpha - \xi_B + \alpha\xi_B)}, h_{CD} \geq \frac{\xi_D \sigma_D^2}{p_C(1 - \alpha)}\}. \tag{64}$$

We can see that the expression of P_3 is segmented by α . If $\frac{\xi_B \sigma_D^2}{p_C(\alpha - \xi_B + \alpha \xi_B)} \geq \frac{\xi_D \sigma_D^2}{p_C(1 - \alpha)}$, which is equivalent to $\frac{\xi_B}{1 + \xi_B} < \alpha \leq \frac{\xi_B \xi_D + \xi_B}{\xi_B \xi_D + \xi_B + \xi_D}$, P_3 can be computed as

$$\begin{aligned} P_3 &= \int_{\frac{\xi_B \sigma_D^2}{p_C(\alpha - \xi_B + \alpha \xi_B)}}^{+\infty} \frac{1}{\varphi_{CD}} e^{-\frac{h_{CD}}{\varphi_{CD}}} dh_{CD} \\ &= \exp \left[-\frac{\xi_B \sigma_D^2}{\varphi_{CD} p_C(\alpha - \xi_B + \alpha \xi_B)} \right]. \end{aligned} \quad (65)$$

Otherwise, we have

$$\begin{aligned} P_3 &= \int_{\frac{\xi_D \sigma_D^2}{p_C(1 - \alpha)}}^{+\infty} \frac{1}{\varphi_{CD}} e^{-\frac{h_{CD}}{\varphi_{CD}}} dh_{CD} \\ &= \exp \left[-\frac{\xi_D \sigma_D^2}{\varphi_{CD} p_C(1 - \alpha)} \right] \end{aligned} \quad (66)$$

for $\frac{\xi_B \xi_D + \xi_B}{\xi_B \xi_D + \xi_B + \xi_D} < \alpha \leq 1$. The proof of Theorem 2 ends here.

APPENDIX C

PROOF OF LEMMA 2

Depending on the relation between \bar{p}_C and P_C , Lemma 1 can be proved by separately proving (26) and (27).

1) *Proof of (26)*: We use contradiction to prove (26). Assuming $R_{SC}(\alpha^*, p_C^*) > R_{CD,S}(\alpha^*, p_C^*)$ for $\bar{p}_C < P_C$, and then there must exist a small enough $0 < \Delta p_C < P_C - \bar{p}_C$ which satisfies $R_{SC}(\alpha^*, p_C^* + \Delta p_C) > R_{CD,S}(\alpha^*, p_C^* + \Delta p_C)$. Hence, we have $R_D(\alpha^*, p_C^*) = R_{CD,S}(\alpha^*, p_C^*)$. Since $R_B(\alpha, p_C)$ and $R_{CD,S}(\alpha, p_C)$ are increasing functions of p_C for a given α , we have $R_B(\alpha^*, p_C^*) < R_B(\alpha^*, p_C^* + \Delta p_C)$ and $R_{CD,S}(\alpha^*, p_C^*) < R_{CD,S}(\alpha^*, p_C^* + \Delta p_C)$, which suggests that $R_{\min}(\alpha^*, p_C^* + \Delta p_C) > R_{\min}(\alpha^*, p_C^*)$ and contradicts with the original assumption of the optimality of (α^*, p_C^*) . Therefore, (26) is proved.

2) *Proof of (27)*: Similar to the proof of (26), we first assume $R_{SC}(\alpha^*, p_C^*) < R_{CD,S}(\alpha^*, p_C^*)$ for $\bar{p}_C \geq P_C$. Then after some algebraic deduction, we know that the optimal transmit power p_C must satisfy $p_C^* > \bar{p}_C$, which is in the infeasible field of $\mathcal{OP}2$. Therefore, (27) is proved and the proof of Lemma 2 is completed.

REFERENCES

- [1] A. Asadi, Q. Wang, and V. Mancuso, "A survey on device-to-device communication in cellular networks," *IEEE Commun. Surveys Tuts.*, vol. 16, no. 4, pp. 1801–1819, 4th Quart., 2014.
- [2] L. Song, D. Niyato, Z. Han, and E. Hossain, *Wireless Device-to-Device Communications and Networks*. Cambridge, U.K.: Cambridge Univ. Press, 2015.

- [3] M. N. Tehrani, M. Uysal, and H. Yanikomeroglu, "Device-to-device communication in 5G cellular networks: challenges, solutions, and future directions," *IEEE Commun. Mag.*, vol. 52, no. 5, pp. 86–92, May 2014.
- [4] A. Tang, X. Wang, and C. Zhang, "Cooperative full duplex device to device communication underlying cellular networks," *IEEE Trans. Wireless Commun.*, vol. 16, no. 12, pp. 7800–7815, Dec. 2017.
- [5] S. Shalmashi and S. B. Slimane, "Cooperative device-to-device communications in the downlink of cellular networks," in *IEEE Wireless Commun. Netw. Conf. (WCNC)*, Istanbul, Turkey, Apr. 2014, pp. 2265–2270.
- [6] P. Popovski and E. De Carvalho, "Improving the rates in wireless relay systems through superposition coding," *IEEE Trans. Wireless Commun.*, vol. 7, no. 12, pp. 4831–4836, Dec. 2008.
- [7] J. Blomer and N. Jindal, "Transmission capacity of wireless ad hoc networks: Successive interference cancellation vs. joint detection," in *Proc. IEEE Int. Conf. Commun. (ICC)*, Dresden, Germany, Jun. 2009, pp. 1–5.
- [8] Y. Cao, T. Jiang, and C. Wang, "Cooperative device-to-device communications in cellular networks," *IEEE Wireless Commun.*, vol. 22, no. 3, pp. 124–129, Jun. 2015.
- [9] Y. Pei and Y.-C. Liang, "Resource allocation for device-to-device communications overlaying two-way cellular networks," *IEEE Trans. Wireless Commun.*, vol. 12, no. 7, pp. 3611–3621, Jun. 2013.
- [10] F. Wang, C. Xu, L. Song, Q. Zhao, X. Wang, and Z. Han, "Energy-aware resource allocation for device-to-device underlay communication," in *Proc. IEEE Int. Conf. Commun. (ICC)*, Budapest, Hungary, Jun. 2013, pp. 6076–6080.
- [11] F. Wang, C. Xu, L. Song, Z. Han, and B. Zhang, "Energy-efficient radio resource and power allocation for device-to-device communication underlying cellular networks," in *Proc. Int. Conf. Wireless Commun. Signal Process. (WCSP)*, Huangshan, China, Oct. 2012, pp. 1–6.
- [12] L. Song, R. Wichman, Y. Li, and Z. Han, *Full-Duplex Communications and Networks*. Cambridge, U.K.: Cambridge Univ. Press, 2017.
- [13] Z. Zhang, X. Chai, K. Long, A. V. Vasilakos, and L. Hanzo, "Full duplex techniques for 5G networks: self-interference cancellation, protocol design, and relay selection," *IEEE Commun. Mag.*, vol. 53, no. 5, pp. 128–137, May 2015.
- [14] L. Song, Y. Li, and Z. Han, "Resource allocation in full-duplex communications for future wireless networks," *IEEE Wireless Commun.*, vol. 22, no. 4, pp. 88–96, Aug. 2015.
- [15] M. Duarte, C. Dick, and A. Sabharwal, "Experiment-driven characterization of full-duplex wireless systems," *IEEE Trans. Wireless Commun.*, vol. 11, no. 12, pp. 4296–4307, Nov. 2012.
- [16] S. Ali, N. Rajatheva, and M. Latva-aho, "Effect of interference of full-duplex transmissions in underlay device-to-device communication," in *Proc. IEEE Canadian Workshop on Inf. Theory (CWIT)*, St. John's, NL, Canada, Sep. 2015, pp. 54–57.
- [17] X. Chai, T. Liu, C. Xing, H. Xiao, and Z. Zhang, "Throughput improvement in cellular networks via full-duplex based device-to-device communications," *IEEE Access*, vol. 4, pp. 7645–7657, Oct. 2016.
- [18] R. Tang, J. Zhao, H. Qu, and Z. Zhang, "Energy-efficient resource allocation for 5G full-duplex enabled device-to-device communication," in *Proc. IEEE Glob. Telecommun. Conf. (GLOBECOM)*, Washington, DC, USA, Feb. 2016, pp. 1–7.
- [19] Z. Zhang, Z. Ma, M. Xiao, Z. Ding, and P. Fan, "Full-duplex device-to-device-aided cooperative nonorthogonal multiple access," *IEEE Trans. Veh. Tech.*, vol. 66, no. 5, pp. 4467–4471, Aug. 2017.
- [20] Z. Ding, M. Peng, and H. V. Poor, "Cooperative non-orthogonal multiple access in 5G systems," *IEEE Commun. Lett.*, vol. 19, no. 8, pp. 1462–1465, Aug. 2015.
- [21] L. Zhang, J. Liu, M. Xiao, G. Wu, Y.-C. Liang, and S. Li, "Performance analysis and optimization in downlink NOMA systems with cooperative full-duplex relaying," *IEEE J. Sel. Areas Commun.*, vol. 35, no. 10, pp. 2398–2412, Jul. 2017.
- [22] G. Zhang, K. Yang, P. Liu, and J. Wei, "Power allocation for full-duplex relaying-based D2D communication underlying cellular networks," *IEEE Trans. Veh. Technol.*, vol. 64, no. 10, pp. 4911–4916, Oct. 2015.

- [23] H. Dun, F. Ye, and Y. Li, "Transmission power adaption for full-duplex relay-aided device-to-device communication," *Symmetry*, vol. 9, no. 3, p. 38, Mar. 2017.
- [24] G. Zhang, K. Yang, P. Liu, and Y. Du, "Using full duplex relaying in device-to-device (D2D) based wireless multicast services: a two-user case," *Sci. China Inf. Sci.*, vol. 58, no. 8, pp. 1–7, Dec. 2015.
- [25] Z. Lin, Y. Li, S. Wen, Y. Gao, X. Zhang, and D. Yang, "Stochastic geometry analysis of achievable transmission capacity for relay-assisted device-to-device networks," in *Proc. IEEE Int. Conf. Commun. (ICC)*, Sydney, NSW, Australia, Aug. 2014, pp. 2251–2256.
- [26] Y. Yang, Y. Zhang, L. Dai, J. Li, S. Mumtaz, and J. Rodriguez, "Transmission capacity analysis of relay-assisted device-to-device overlay/underlay communication," *IEEE Trans. Ind. Inform.*, vol. 13, no. 1, pp. 380–389, Oct. 2017.
- [27] R. Ma, Y.-J. Chang, H.-H. Chen, and C.-Y. Chiu, "On relay selection schemes for relay-assisted D2D communications in LTE-A systems," *IEEE Trans. Veh. Tech.*, vol. 66, no. 9, pp. 8303–8314, Mar. 2017.
- [28] R. Ma, N. Xia, H.-H. Chen, C.-Y. Chiu, and C.-S. Yang, "Mode selection, radio resource allocation, and power coordination in D2D communications," *IEEE Wireless Commun.*, vol. 24, no. 3, pp. 112–121, Feb. 2017.
- [29] M. Hasan, E. Hossain, and D. I. Kim, "Resource allocation under channel uncertainties for relay-aided device-to-device communication underlaying LTE-A cellular networks," *IEEE Trans. Wireless Commun.*, vol. 13, no. 4, pp. 2322–2338, Mar. 2014.
- [30] M. Hasan and E. Hossain, "Distributed resource allocation for relay-aided device-to-device communication: A message passing approach," *IEEE Trans. Wireless Commun.*, vol. 13, no. 11, pp. 6326–6341, Jul. 2014.
- [31] S. Kishk, N. Almofari, and F. Zaki, "Distributed resource allocation in D2D communication networks with energy harvesting relays using stable matching," *Ad Hoc Netw.*, vol. 61, pp. 114–123, Jun. 2017.
- [32] A. Al-Hourani, S. Kandeepan, and E. Hossain, "Relay-assisted device-to-device communication: A stochastic analysis of energy saving," *IEEE Trans. Mobi. Computing*, vol. 15, no. 12, pp. 3129–3141, Jan. 2016.
- [33] S. Dang, G. Chen, and J. P. Coon, "Outage performance analysis of full-duplex relay-assisted device-to-device systems in uplink cellular networks," *IEEE Trans. Veh. Tech.*, vol. 66, no. 5, pp. 4506–4510, May 2017.
- [34] S. Dang, J. P. Coon, and G. Chen, "Resource allocation for full-duplex relay-assisted device-to-device multicarrier systems," *IEEE Wireless Commun. Lett.*, vol. 6, no. 2, pp. 166–169, Apr. 2017.
- [35] B. Ma, H. Shah-Mansouri, and V. W. S. Wong, "A matching approach for power efficient relay selection in full duplex D2D networks," in *Proc. IEEE Int. Conf. Commun. (ICC)*, Kuala Lumpur, Malaysia, May 2016, pp. 1–6.
- [36] A. Memmi, Z. Rezki, and M. S. Alouini, "Power control for D2D underlay cellular networks with channel uncertainty," *IEEE Trans. Wireless Commun.*, vol. 16, no. 2, pp. 1330–1343, Feb. 2017.
- [37] I. Krikidis and H. A. Suraweera, "Full-duplex cooperative diversity with Alamouti space-time code," *IEEE Wireless Commun. Lett.*, vol. 2, no. 5, pp. 519–522, Oct. 2013.
- [38] L. J. Rodríguez, N. H. Tran, and T. Le-Ngoc, "Performance of full-duplex AF relaying in the presence of residual self-interference," *IEEE J. Sel. Areas Commun.*, vol. 32, no. 9, pp. 1752–1764, Sep. 2014.
- [39] L. J. Rodríguez, N. H. Tran, and T. Le-Ngoc, "Optimal power allocation and capacity of full-duplex AF relaying under residual self-interference," *IEEE Wireless Commun. Lett.*, vol. 3, no. 2, pp. 233–236, Feb. 2014.
- [40] K. J. Arrow and A. C. Enthoven, "Quasi-concave programming," *Econometrica*, vol. 29, no. 4, pp. 779–800, Oct. 1961.
- [41] B. Radunović and J.-Y. L. Boudec, "A unified framework for max-min and min-max fairness with applications," *IEEE/ACM Trans. Netw.*, vol. 15, no. 5, pp. 1073–1083, Oct. 2007.
- [42] V. Bergelson and A. Leibman, "Distribution of values of bounded generalized polynomials," *Acta Mathematica*, vol. 198, no. 2, pp. 155–230, Jun. 2007.

- [43] G. Jameson, “Counting zeros of generalised polynomials: Descartes’ rule of signs and Laguerre’s extensions,” *The Mathematical Gazette*, vol. 90, no. 518, pp. 223–234, Jul. 2006.
- [44] R. L. Burden and J. D. Faires, *Numerical Analysis*. Pacific Grove, CA, USA: Brooks-Cole, 2001.